PERFORMANCE OF ABSORPTION HEAT PUMP USING FINE PARTICLE SLURRY OF LIBR CRYSTAL

Yoshinori Itaya*[1], Nobuhisa Ichihashi[2], Koichi Nagatani[1] and Nobusuke Kobayashi[2]
*Author for correspondence
1 Department of Mechanical Systems Engineering,
Gifu University,
Gifu, 501-1193,
Japan,
E-mail: yitaya@gifu-u.ac.jp
2 Department of Chemical Engineering,
Nagoya University,
Nagoya, 464-8603,
Japan

ABSTRACT

Absorption heat pump systems (AHP) are one candidate of attractive technologies to upgrade and utilize exhaust heat of low temperature level for refrigeration or heating up without emitting global warming gas. This work is to propose the method to form fine-particle slurry of LiBr crystal and to evaluate the effectiveness of the slurry for advancement of the absorption performance in LiBr/water AHP. It was found that the fine particle slurry of LiBr crystal is formed stably in the solution under a super saturation condition when zeolite powder is suspended. This phenomenon is considered to take place since the crystal grows around the zeolite particles by a function as nucleus. Then almost saturated concentration is maintained due to dissolution of the crystal even if the solution is diluted by absorption of water vapor in the absorber. The theoretical analysis based on heat and mass transfer model predicted that the output power of AHP was improved up to twice when compared with the conventional solution in lower concentration than saturation solubility without containing any fine powder of adsorbent or crystal. The measurement of the slurry properties and experiment on heat transfer of slurry film flowing on a heat transfer plate was carried out, and the effectiveness of the slurry as well as the reasonability of the modeling was confirmed.

INTRODUCTION

Reduction of primary energy consumption would be the first issue that should be implemented to mitigate significantly carbon dioxide emission represented as greenhouse gas. Now a day, a huge amount of heat at lower temperature than 100 °C is wasted into the atmosphere. Hence R&D on recovery of such low rank energy is essential and important for effective utilization of energy. Adsorption heat pump (AHP) is an effective technology for upgrading waste heat in a form of refrigeration, and has been commercialized in industries.

NOMENCLATURE

A	[m^2]	Heat transfer surface area
a	[kg-sol /kg-ads]	Equilibrium adsorption parameter defined by Eq. (7)
b	[kg-LiBr /kg-ads]	Equilibrium adsorption parameter defined by Eq. (7)
C_{LiBr}	[kg-LiBr /kg-sol]	LiBr concentration in solution
c_{pa}	[J/(kg-ads·K)]	Specific heat of adsorbent
c_{pLiBr}	[J/(kg-LiBr·K)]	Specific heat of LiBr crystal
h_s	[J/kg-sol]	Enthalpy of solution
h_w	[W/(m^2·K)]	Overall heat transfer coefficient
k_p	[kg/(m^2·s Pa)]	Mass transfer coefficient
L_e	[J/kg]	Latent heat of water vapor
$\dot{m}$	[kg-water /(m^2·s)]	Rate of absorption or evaporation
P_{evap}	[Pa]	Vapor pressure in evaporator or condenser
P_s	[Pa]	Equilibrium vapor pressure
Q	[W]	Heat exchange rate
q^*	[kg-LiBr /kg-ads]	Equilibrium adsorption amount of LiBr in adsorbent per unit adsorbent
q_{cond}	[W/m^2]	Phase change enthalpy per unit heat transfer surface area
q_w	[W/m^2]	Heat transfer rate between working fluids and solution
T	[K]	Solution temperature
T_w	[K]	Heat transfer fluid temperature
w	[kg-sol/s]	Flow rate of solution
w_c	[kg-ads	Flow rate of adsorbent in solution

There are some types of AHP by combination of absorbents and working fluids [1,2]. Ammonia/water and lithium bromide/water systems are representative AHP; the former one is suitable for recovery of relatively low temperature heat but the performance is greatly dependent on distillation to separate ammonia and water in the generator, and only a little room of R&D for innovation is remaining. On the other hand, in the latter system combustion gas at high temperature is used mostly in the generator and recovery of lower temperature level of heat than 100 °C has been quite limited conventionally, but more choice of absorbents will be available to improve the performance. Recent researches of lithium bromide/water AHP have been focused on evaluation of COP and exergy for refrigeration and heating up [3], modeling or optimization for the system design [4,5], utilization of renewable energy such as biomass [6], solar energy [7] and low level heat sources [8]. Several researches on absorbent have been also reported to maintain high concentration of the solution and advance absorption performance of water vapor by addition of third component into lithium bromide/water solution because lower concentration of the solution results in falling down absorptivity of vapor into the solution causing reduction of AHP performance due to elevation of the equilibrium vapor pressure. The representative example of the additives are $ZnCl_2$-$CaBr_2$ [9], $HO(CH_2)_3OH$ or LiI-$LiCl$-$LiNO_3$ [10], CH_3COO or $CH_3CH(OH)COONa$ [11], CHO_2Na, CHO_2K, CH_3CO_2, $CH_3CH(OH)CO_2Na$ [12] and n-octanol [13]. There was also a report to use H_2O-$NaOH$-KOH-$CsOH$ system as an alternate adsorbent of $LiBr/H_2O$ system [14]. Their additives employed are salts, organic compounds or surfactants.

Itaya et al. [15] proposed to disperse a fine powder of adsorbent like activated carbon and zeolite into the $LiBr/H_2O$ solution. The adsorbent acts as adsorber of LiBr in the solution slurry. The amount of equilibrium adsorption of a soluble component, i.e lithium bromide here, is dependent generally on the concentration in the solution. The adsorbed component is desorbed and reduction of the concentration is relaxed even if the solution absorbs water vapor. As the result, they found analytically the improvement of the AHP performance. In the progress they noticed additionally that a fine particle slurry of LiBr crystal could be formed in the solution when the suspension of the solution and the fine powder achieved at a super saturation state of the soluble salt. If this phenomenon is applied to the absorbent of LiBr/water AHP, it may be made possible to operate the AHP in so high concentration as the super saturation state beyond the solubility of LiBr without causing a problem of blockage due to crystal growth.
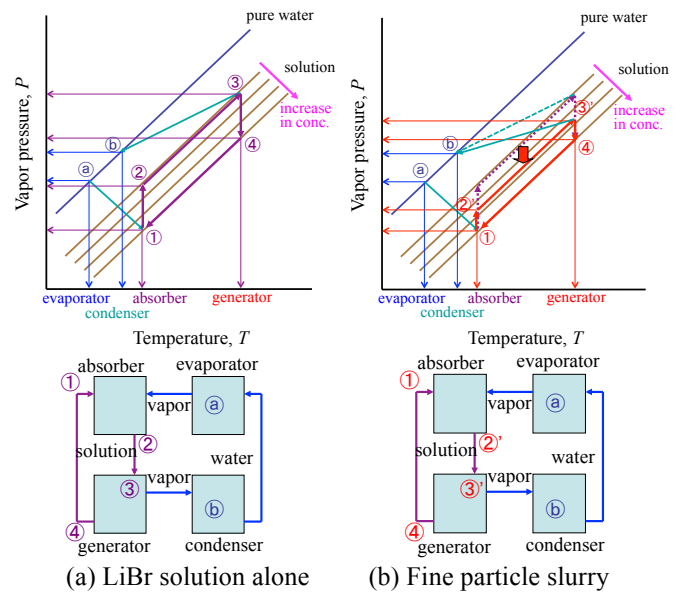

Figure 1 Comparison of the operation on *P-T* chart between LiBr solution only and the slurry in AHP system

The present study is to evaluate the effectiveness of fine-particle slurry of LiBr crystal as an absorption solution of AHP. The properties of the slurry were measured preliminarily to elucidate the behavior of slury formation. The effect of fine particle suspension of adsorbent and LiBr crystal on the performance of AHP was examined by a modeling based on heat and mass transfer. In addition, the experiment on heat transfer between a heating fluid and a film of solution/adsorbent suspension slurry flowing on a tilted flat heat transfer plate was carried out to confirm the validity of the modeling.

PRINCIPLE OF AHP PERFORMANCE IMPROVEMENT

The conceptual principle to improve AHP performance by the fine particle slurry of adsorbent and LiBr crystal is drawn in Figure 1. The states expressed by symbol in AHP system consisting of absorber, generator, evaporator and condenser correspond to the ones on the chart of equilibrium vapor pressure of the solution in each concentration *P* against temperature *T*. In general the equilibrium pressure falls with increase in the concentration of the solution. The state on the *P-T* chart cycles along the path in the order of ①=>②=>③=>④ according to circulation of the solution between absorber and generator. When fine particles of adsorbent or LiBr crystal are suspended in the solution, the operation can be made possible along the path of ②' and ③' whose concentration of the solution is higher than the case of the solution only if it is compared at the same amount of water vapor absorbed in absorber as seen in Figure 1(b) because of desorption of LiBr adsorbed in adsorbent powder or dissolution of LiBr crystal particles in to the solution. The absorption rate of water vapor into the solution is given by vapor pressure difference between ⓐ in evaporator and ② or ②' in absorber as the driving force.

Hence the absorption rate would be enhanced in the slurry where the pressure difference becomes greater than in the solution only.

THEORETICAL MODEL

The outline of the theoretical model in absorber is shown in Figure 2. The absorbent solution flows down forming a thin film on a heat transfer plate and absorbs water vapor from evaporator. Heat generated by absorption of vapor is exchanged with cooling water flowing along the opposite side of the plate. In generator, hot heating fluid flows in stead of cooling water and the heat and mass transfer takes place in the inverse direction, but the model can be represented in quite same form as that in absorber.
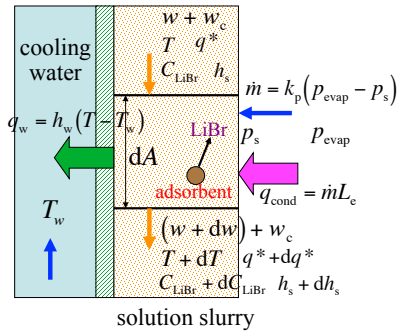

Figure 2 Outline of analytical model

In the present analysis, the assumptions are introduced as:
1) The solution is flowing down with a uniform thickness of the film on a heat transfer plate.
2) Temperature and concentration profiles are uniform in the direction of film thickness.
3) Vapor pressure on the solution film is maintained in the saturation state at the concentration and temperature.
4) The rates of absorption and evaporation are proportional to the driving force given by the vapor pressure difference between on the solution film surface and in evaporator/condenser.
5) Vapor pressure in evaporator and condenser is approximated by the saturation pressure of pure water at the temperature in each vessel.
6) Cooling or heating fluid flows in parallel or counter direction against the flow of the solution film.
7) Heat transfer rate between the solution and cooling or heating fluid is given by multiplying a overall heat transfer coefficient and the temperature difference between the solution film and fluid.
8) Adsorption amount of LiBr into adsorbent is equilibrium to the concentration in the solution if the concentration is lower than the saturation solubility.
9) The concentration of the solution is maintained at the saturation solubility if it is in the super saturation state.
10) Heat loss is negligibly small.
11) Evaporator and condenser are maintained at each constant temperature set.

12) Heat transfer and diffusion of LiBr is ignored in the flow direction of the solution.

The conservation equations of mass and energy transfer are formulated under those assumptions

LiBr:

$$-w_c \frac{dq*}{dA} = \frac{d(wC_{LiBr})}{dA} \tag{1}$$

Water:

$$\frac{d\{w(1-C_{LiBr})\}}{dA} = \dot{m} \tag{2}$$

Energy:

$$\frac{d\left(h_s w + c_{pa} w_c T + c_{pLiBr} w_c \phi T\right)}{dA} + q_w = q_{cond} \tag{3}$$

These equations represent changes along the surface area of the heat transfer plate. The rates of vapor absorption or evaporation and heat transfer are expressed by, respectively

$$\dot{m} = k_p\left(p_{evap} - p_s\right) \tag{4}$$

$$q_w = h_w\left(T - T_w\right) \tag{5}$$

Latent heat enthalpy due to phase change q_{cond} is given by

$$q_{cond} = \dot{m}L_e \tag{6}$$

The LiBr amount crystallized or adsorbed on adsorbent powder ϕ was given by the equilibrium adsorption amount $q*$ as approximation in Eq. (7) if the concentration is less than saturation solubility.

$$\phi = q* = aC_{LiBr} + b \quad \text{for } C_{LiBr} < C*_{LiBr} \tag{7}$$

Indeed the correlation was confirmed with a=1.5 and b=0 for a zeolite powder by measurement [15]. If the concentration of the solution is in the super saturation state, ϕ was determined in Eq. (1) by letting C_{LiBr} constant as

$$C_{LiBr} = C*_{LiBr} \quad \text{for } C_{LiBr} \geq C*_{LiBr} \tag{8}$$

The fundamental equations were solved numerically by integration along the surface area of the heat transfer plate in absorber or generator. The analysis was also performed for a closed-cycle system as the solution circulates between absorber and generator. Then the calculation in absorber and generator was repeated sequentially until relaxing to a sufficient accuracy of relative error 10^{-10}. The properties of LiBr/water solution were cited from references [1,3-5].

EXPERIMENTS

Preparation of Slurry Sample

The sample of the LiBr solution slurry was prepared by the following procedure. Lithium bromide reagent (SIGMA-

ALDRICH, purity >99%) was dissolved in deionized water at first. Then temperature of the solution rose up to about 80 °C by generation of dissolution heat. The solution of 63.4% in LiBr concentration was cooled with stirring after adding and suspending zeolite powder (Tosoh, HSZ-320-NAA) by 5.56%. The fine particle of LiBr crystal began generating in the solution and the slurry was formed as seen in Figure 3(a) when the concentration achieved at a super saturation state. On the other hand, a large lump of the crystal was grown up as seen in Figure 3(b) unless any zeolite powder is suspended.

(a) Fine particle slurry of LiBr   (b) LiBr crystal lump grown

Figure 3 Pictures of LiBr fine particle slurry and crystal lump grown in the solution.

Measurement of Properties

The particle size distribution and viscosity were measured as properties of the slurry prepared in the above. The size distribution was determined under the temperature at 25 °C by laser diffraction/scattering type of particle size analyser (Horiba, LA-920). Viscosity of the slurry was measured by using rotational viscometer (Haake, VT550). The amount of LiBr crystal was varied by controling temperature of the slurry.

Heat Transfer Experiment

Overall heat transfer coefficients between a heat transfer working fluid and a solution/zeolite suspension film flowing on the tilted plate were determined experimentally and the temperatures of the film was compared with the result of numerical analysis based on the theoretical modeling. The present experiment was performed representatively in the heat transfer system where water vapor evaporates on the surface of the film flowing on a heating flat plate whose opposite side is exposed by a hotter working fluid than the solution so to work as a heating condition of heat exchange.

Figure 4 shows the outline of heat transfer experimental setup. The solution of LiBr/water or LiBr/water/zeolite suspension stored in the upper tank was fed constantly at each specified rate to flow in forming a film on the surface of a flat heat transfer plate in the test duct. The flow rate was regulated by diaphragm pump. The exit solution was discharged into the lower storage tank. Zeolite used here was same HSZ-320-NAA as that described in the sample preparation. Silicone oil (Shin-Etsu Chemical, KF-96-100CS) was employed for the heat transfer working fluid, and supplied to the bottom of the duct in a counter flow against the solution flow direction. The oil was

maintained stably at 90 °C in the thermostatic bath. The heat transfer plate was made of SUS329J4L stainless steel with the effective size, 1,002 mm in length, 102 mm in width and 3 mm in thickness, and its surface was treated so to form a uniform solution film over the surface by hydrophilic ceramic coating (Shinko, Belath Coat). The plate was tilted at an angle of 4.57°. The upper room of the solution side in the duct was evacuated and joined to a plate heat exchanger type of condenser refrigerated by cold water from the chiller. Temperatures were measured by thermocouples placed at the inlet and outlet of the both fluids of the solution and silicone oil. The water evaporation rate on the film surface was determined from the difference of LiBr concentration between the inlet and outlet solutions. The LiBr concentration was measured from the weight of remain dried up in dryer at 200 °C.
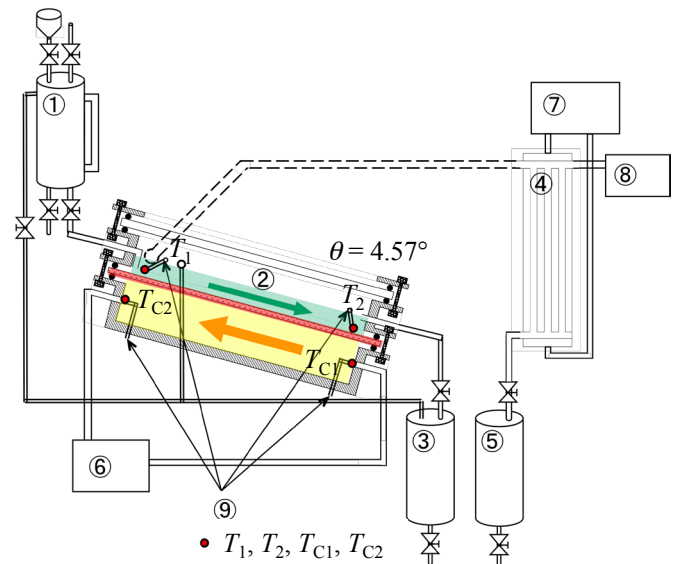
① Upper solution storage tank   ② Test duct of heat transfer experiment   ③ lower solution storage tank   ④ Condenser   ⑤ Condensed water storage tank   ⑥ Thermostatic bath   ⑦ Chiller   ⑧ Vacuum pump   ⑨ Thermocouples

Figure 4 Experimental setup of heat transfer

BEHAVIOR OF CRYSTAL FINE PARTICLE SLURRY FORMATION AND ITS PROPERTIES

The particle size distribution of LiBr crystal in the slurry sample is shown in Figure 5. The solid and dashed lines represent the distribution of the LiBr crystal particles and the zeolite, respectively. The size of the crystal particles was distributed in the range of 10 to 200 μm while 2 to 10 μm for zeolite, and only a little fraction of the crystal particle was observed in the size overlapping with the zeolite. The result seems that the crystal is generated around the particle(s) of zeolite by acting as a seed of nucleus under the super saturation state. The median size of the crystal particle can be estimated to be 7.45 μm, supposed that the crystal grows uniformly around each one particle of zeolite whose median size is 7.09 μm. This

estimated size was too small to compare with that measured as seen in Figure 4. The fact means that coalescence of some particles might occur in the progress of crystal growth and/or the crystal couldn't be grown uniformly in continuous solid free from any pore or gap. However, the size would be sufficiently small to handle the slurry without causing blockage of the solution stream during the operation.
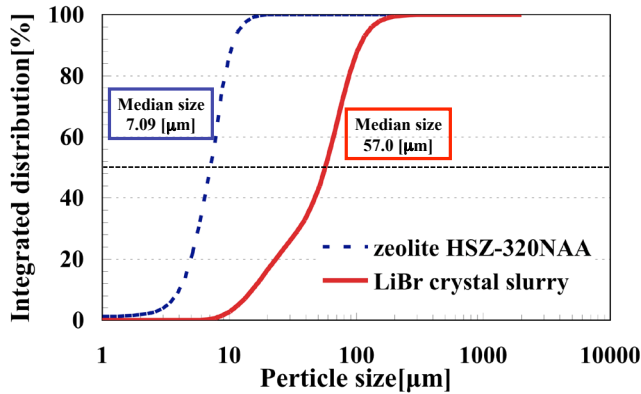

Figure 5 Particle size distribution of LiBr crystal in the slurry and zeolite

Figure 6 shows viscosity of the slurry against the amount of LiBr crystal. Viscosities of pure water at 20 °C and LiBr solution of 63.4% in concentration at 50 °C (free from LiBr crystal) are also compared in the graph. The solution containing no particle was 6 times as viscous as water, and viscosity of the solution was raised additionally by 1.5 times due to suspension of only the zeolite in 5.56 %. When the temperature of the solution containing zeolite falls down at 35 and 20 °C, the slurry of LiBr crystal particles is formed and the viscosity increases up to almost twice for 35 °C and 2.8 times for 20 °C of the original solution without any solid particle. The slurry was confirmed to keep sufficient fluidity in the range of the present level of fine particle contents and temperatures in the slurry.
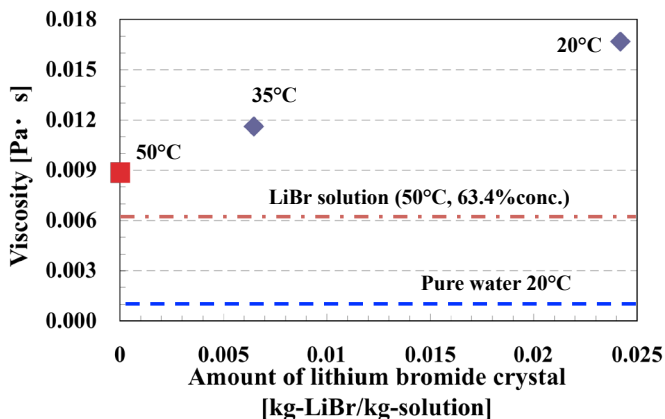

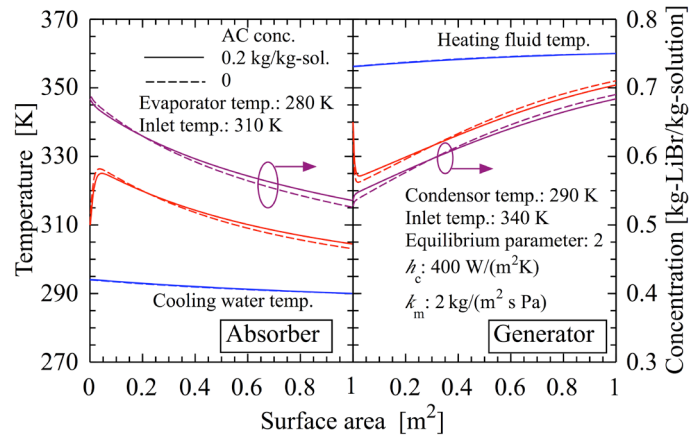**Figure 6** Viscosity of the slurry in different contents of LiBr crystal particles

Figure 7 Profiles of temperature and LiBr concentration in the solution/adsorbent suspension and the only solution in closed loop system

ANAYTICAL RESULTS

Effect of Solution/Adsorbent Suspension

Figure 7 shows an example of numerical analyses on temperature and LiBr concentration profiles in a film of the solution along the surface area of the heat transfer plate, which is corresponding to the flow direction. The profiles are compared between the solution/adsorbent suspension and only the solution to study the effect of adsorption/desorption of LiBr by adsorbent under a condition free from LiBr crystal particle generation for the closed loop system of each suspension or solution in absorber and generator. The total surface area of a heat transfer plate was assumed as 1 m^2 both in absorber and generator. The initial set conditions of this analysis were 0.01 kg-solution/s in flow rate, 0.7 kg-LiBr/kg-solution in LiBr concentration, 0.2 kg-AC/kg-solution in adsorbent content, 0.5 kg/s in flow rate of heat transfer working fluid, 290 and 360 K in inlet working fluid temperature in absorber and generator, 280 and 290 K in temperature of evaporator and condenser respectively, but the concentration and flow rate of the solution are changed to converge in the relaxation step of analysis. Temperatures of the inlet solution were fixed at 310 K in absorber and 340 K in generator. The overall heat transfer coefficient and mass transfer coefficient were applied tentatively at 400 W/(m^2·K) and 2 kg/(m^2·s·Pa), respectively.

The temperatures rise immediately due to absorption of water vapor as soon as the solution enters in absorber while fall down in generator due to vaporization, and sequentially the solution is cooling or heating gradually by the heat exchange through the heat transfer plate. The suspension maintains higher LiBr concentration at the outlet in absorber than the solution without adsorbent due to the effect of adsorption although the concentration of the solution generated or at the inlet in absorber trends lower. Indeed the absorption rate of water vapor or the output of AHP in absorber is enhanced by 5 to 5.5 % as seen in Figure 8 as far as the analyses are performed for any mass transfer coefficient in the range of 2 to 4

kg/(m^2·s·Pa). The absorption rate of the suspension is normalized by one of the only solution. It should be noted that the mass transfer coefficient influences the output only a little.
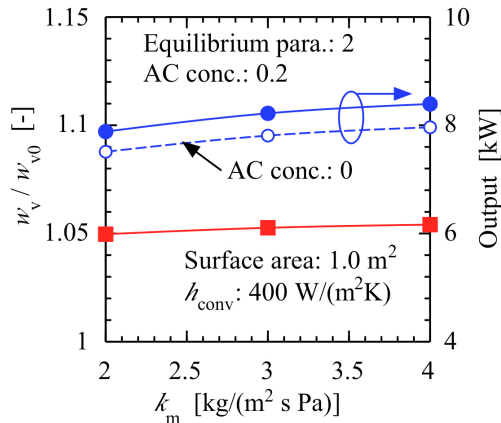

Figure 8 Effect of mass transfer coefficient on water vapor absorption rate and output of AHP

Figure 9 Effect of LiBr crystal fine particle slurry on water vapor absorption rate

Effect of LiBr Crystal Slurry

The analysis was performed in the open system to fundamentally evaluate AHP performance in the case where the fine particle slurry of LiBr crystal is employed as the absorption solution. Figure 9 shows the absorption rate of water vapor against the surface area of the heat transfer plate in absorber. The absorption rate is defined by the rate absorbed in the test section from the inlet to the specified surface area. It was assumed that a sufficient LiBr crystal exists in the slurry. The analytical results on the solution/zeolite suspension and the only solution are also compared in the figure. The inlet LiBr concentration was set at 64 %. The other parameters required for the analyses were adopted to be the same as those used in Figure 7. The absorption rate in the slurry is enhanced almost twice of the only solution without any particle in the test section 1 m^2 while that in the solution/zeolite suspension is 20 %. The result implies that the performance of AHP is expected to be greatly advanced due to the effect of excellent hygroscopicity of the solution preserved at high concentration by dissolution of salt crystal if the slurry is introduced.

EXPERIMENTAL RESULT OF HEAT TRANSFER

Heat Transfer Coefficient

Performance of AHP is dependent on the heat exchange rate of the solution to approximate the operation temperature as close as possible though it was not influenced so much on the mass transfer coefficient in pointed out in Figure 8. Thus the heat transfer coefficient between the working fluid and the solution/zeolite suspension film flowing on a flat heat transfer plate was examined prior to evaluate the validity of the present modeling.

The overall heat transfer coefficient h_w was defined by
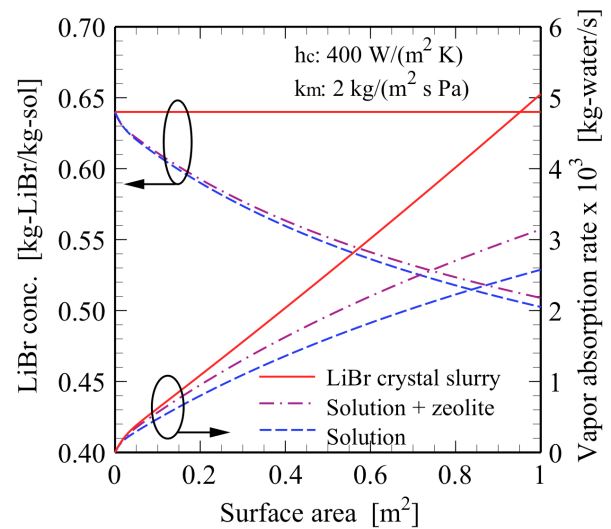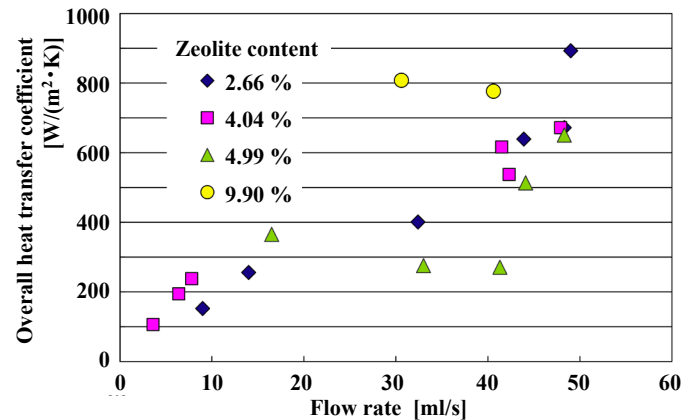
$$Q = h_w A \Delta T_{lm} \qquad (9)$$

Figure 10 Overall heat transfer coefficient between working fluid and soltion/zeolite suspension film flowing on tilted plate

where ΔT_{lm} is logarithm mean temperature difference given by

$$\Delta T_{lm} = \frac{(T_{w1} - T_2) - (T_{w2} - T_1)}{\ln\left[(T_{w1} - T_2)/(T_{w2} - T_1)\right]} \qquad (10)$$

The heat transfer rate is expressed as

$$Q = h_s w + c_{pa} w_c T + w_v L_e \qquad (11)$$

The overall heat transfer coefficient can be determined by applying the temperatures of both the working fluid and the suspension at the inlet and outlet of the test section in the duct, LiBr concentrations in the suspension at the inlet and outlet and the inlet flow rates of both the fluids measured experimentally. The enthalpy of the solution was predicted by a function of the temperature and LiBr concentration [5].

The overall heat transfer coefficient for different concentrations of zeolite in the suspension is plotted to the flow

rate in Figure 10. The heat transfer coefficient trends to rise with the flow rate though the data is scattered a little widely because only a slight difference of the LiBr concentration in the suspension was observed between the inlet and the outlet, which resulted in leading a low accuracy of the heat transfer rate estimated. The zeolite content doesn't affect significantly the heat transfer coefficient. The magnitude of the coefficient employed in the analysis was reasonable as far as compared with this data.

Validity of Modeling

The result of numerical analysis was compared with the experimental data of heat transfer specified in the last section. Figure 11 shows the behavior of LiBr concentration and temperature in solution/zeolite suspension along the surface area of a heat transfer plate. The experimental data is plotted on the surface area corresponding to the effective area of the heat transfer plate, i.e. 0.1 m^2. The result was one obtained for 2.66 % in zeolite content and 9.0 ml/s in the flow rate of the suspension. The analytical result is in sufficient agreement with the experimental data on both the temperature and LiBr concentration at the outlet of the test section in the duct. This agreement will confirm the reasonability of the theoretical model developed in the present study to predict the performance of AHP introducing the slurry or suspension as an absorbent solution.
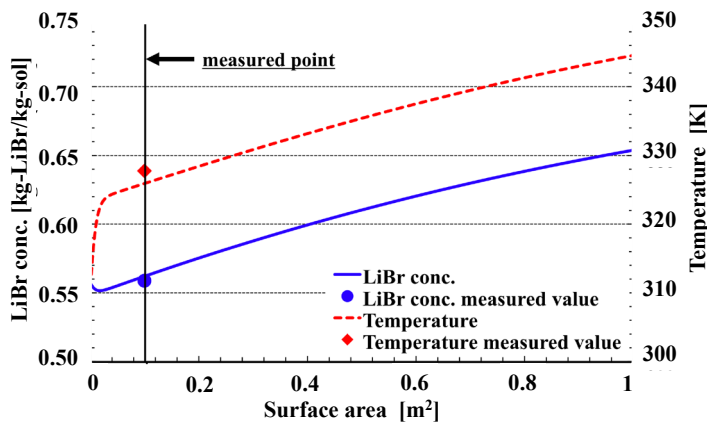

Figure 11 Behavior of LiBr concentration and temperature in solution/zeolite suspension film flowing on a tilted surface

CONCLUSION

Application of fine particle slurry of adsorbent and LiBr crystal into an absorption solution was proposed as a means to enhance the performance of lithium bromide/water AHP. The solution/adsorbent suspension relaxed dilution of the LiBr concentration due to the effect of adsorption and desorption of the salt component into absorbent. The numerical analysis predicted an improvement effect of AHP performance by adsorbent suspension. It was also found that fine particles of LiBr crystal were generated under a super saturation state beyond the solubility if fine powder of zeolite was suspended in

the solution. The size of the crystal particles in the slurry was distributed in the range of 10 to 200 μm, and the slurry, whose viscosity was 2.8 times of 63.4 % LiBr solution without containing any particles, kept a sufficient fluidity. The absorption rate of water vapor in absorber or the output of AHP was advanced significantly up to 100 % as high as that of the only solution from the evaluation by the modeling developed in the present study if this slurry is introduced successfully to AHP. the modeling was verified by a reasonable agreement with the experimental data of heat transfer on a film flow of the solution/zeolite suspension on a tilted flat heat transfer plate.

REFERENCES

[1] Herold K. E., Radermacher R. and Klein S. A.; Adsorption chillers and heat pumps, CRC Press, 1996

[2] Srikhirin P., Aphornratana S. and Chungpaibulpatana S., A review of absorption refrigeration technologies, *Renewable and Sustainable Energy Rev.*, Vol. 5, 2001, pp. 343-372

[3] Sencan A., Yakut K. A. and Kalogirou S. A., Exergy analysis of lithium bromide/water absorption systems, *Renewable Energy*, Vol. 30, 2000, pp. 645-657

[4] Florides G. A., Kalogirou S. A., Tassou S. A. and Wrobel L. C., Design and construction of a LiBr-water absorption machine, *Energy Convers. Manag.*, Vol. 44, 2003, pp. 2483-2508

[5] Sun D. W., Thermodynamic design data and optimum design maps for absorption refrigeration system, *Appl. Therm. Eng.*, Vol. 17, 1997, pp. 211-221

[6] Kai T., Uemura Y., Teraoka Y., Takahashi T., Hatate Y. and Yoshida M., Design and operation of an air-conditioning system fueled by wood pellets, *Renewable Energy*, Vol. 33, 2008, pp. 720-725

[7] Yaxiu G., Yuyuan W. and Xin K., Experimental research on a new solar pump-free lithium bromide absorption refrigeration system with a second generator, *Solar Energy*, Vol. 82, 2008, pp. 33-42

[8] Keil C., Plura S., Radspieler M., and Schweigler C., Application of customized absorption heat pumps for utilization of low-grade heat sources, *Appl. Therm. Eng.*, Vol. 28, 2008, pp. 2070-2076

[9] Iyoki S. and Uemura T., Performance characteristics of the water - lithium bromide - zinc chloride - calcium bromide absorption refrigerating machine, Absorption Heat Pump and Absorption Heat Transformer, *Rev. Int. Froid* (*Int. J. Refrig.*), Vol. **13**, 1990, pp. 191-196

[10] Kim K. S. and Lee H., Differential enthalpies of dilution of the lithium bromide + 1,3-propanediol + water and lithium bromide + lithium iodide + lithium chloride + lithium nitrate + water system, *J. Chem. Eng. Data*, Vol. **47**, 2002, pp. 397-399

[11] De Lucas A., Donate M. and Rodriguez J. F., Vapour pressures, dencities, and viscosities of the (water + lithium bromide + potassium acetate) system and (water + lithium bromide + sodium lactate) system, *J. Chem. Thermodynamics*, Vol. 38, 2006, 123-129

[12] Donate M., Rodriguez L., De Lucas A. and Rodriguez J. F., Thermodynamic evaluation of new absorbent mixtures of lithium

bromide and organic salts for absorption refrigeration machines, *Int. J. Refrig.*, Vol. **29**, 2006, pp. 30-35

[13] Nakoryakov V. E., Grigoryeva N. I., Bufetov N. S. and Dekhtyar R. A., Heat and mass transfer intensification at steam absorption by surfactant additives, *Int. J. Heat and Mass Transfer*, Vol. **51**, 2008, pp. 5175-5181

[14] Romero R. J., Rivera W., Gracia J. and Best R., Theoretical comparison of performance of an absorption heat pump system for cooling and heating operating with an aqueous ternary hyfroxide and water/lithium bromide, *Appl. Therm. Eng.*, Vol. **21**, 2001, pp. 1137–1147

[15] Itaya Y., Ichihashi N. and Kobayashi N., Effect of solution/adsorbent slurry on absorption heat pump performance, Kagaku Kogaku Ronbunshu, Vol. 36, 2010, pp. 505-511